Investigation of the Lead-free Solder Joint Shear Performance

James Webster, Jianbiao Pan[1], Brian J. Toleno
[1]Cal Poly State University
Industrial & Mfg Engineering, San Luis Obispo, CA 93407
Phone: (805) 756-2540, Fax: (805) 756-1420, pan@calpoly.edu

Abstract

Reflow profile has significant impact on solder joint performance because it influences wetting and microstructure of the solder joint. The purpose of this study is to investigate the effects of reflow profile and thermal shock on the shear performance of eutectic SnPb (SnPb) and Sn3.0Ag0.5Cu (SAC305) solder joints. Test boards were assembled with four different sized surface mount chip resistors (1206, 0805, 0603 and 0402). Nine reflow profiles for SAC 305 and nine reflow profiles for SnPb were developed with three levels of peak temperature (12ºC, 22ºC, and 32ºC above solder liquidus temperature, or 230ºC, 240ºC, and 250ºC for SAC 305; and 195ºC, 205ºC, and 215ºC for SnPb) and three levels of time above solder liquidus temperature (30 sec., 60 sec., and 90 sec.). Half of the test vehicles were then subjected to air-to-air thermal shock conditioning from -40 to 125°C. The shear force data were analyzed using the Analysis of Variance (ANOVA). The fracture surfaces were studied using a Scanning Electron Microscopy (SEM) with Energy Dispersive Spectroscopy (EDS). It was found that thermal shock degraded both SnPb and SnAgCu joints shear strength, and that the effect of thermal shock on solder joint shear strength is much more significant than that of reflow profile. The SnAgCu solder joints have weaker shear strength than the SnPb solders. The SnAgCu solder joint after thermal shock retains more of its shear strength than that of SnPb for small components and vice versa for larger components.

Keywords

Lead free solder, shear force, reflow profile, thermal shock

Introduction

The solder joint between the component and the printed circuit board (PCB) should provide not only a reliable electrical interconnection, but also a reliable mechanical interconnection. The transition from through-hole technology to surface mount technology has increased the importance of reliable solder joint shear strength, because the solder joint itself must support a shear force due to mechanical shock and/or thermal stress.

In response to the European Union (EU) Restriction of Hazardous Substances (RoHS) and other countries' lead-free directives, the electronics industry is transiting to lead-free soldering to meet the regulatory requirements to eliminate lead from solders used in consumer electronics products. SnAgCu lead-free solder alloy has been widely adopted as an alternative to eutectic tin-lead (SnPb) solder [1-3]. But the reliability of SnAgCu solder interconnection is still not well understood [4].

It is well known that reflow profile influences wetting and microstructure of the initial solder joint, and thus impact on solder interconnection reliability. Due to the high reflow temperature of SnAgCu, the dissolution of the base metallization on the substrate and components to the lead-free solder is much higher, which impacts the properties of the intermetallic layer. Salam, et al. [5] studied the effects of reflow profile parameters on intermetallic compound (IMC) thickness and microstructure of the SnAgCu solder joints. They found that the most significant factor in achieving a thin IMC layer and fine microstructure is the peak temperature. Oliver, et al. [6] investigated the effect of thermal aging on the shear strength of lead-free solder joints and concluded that the shear strength decreases as the aging time increases. Bukhari, et al. [7] evaluated the effects of assembly process parameters and thermal aging. Their results indicate that the effects of thermal aging on solder joint shear strength are much larger than the effects of assembly process variables.

This paper presents the experimental results on the effects of reflow profile and thermal shock on shear force of both SnPb and SnAgCu solder joints.

Experiment

A five-factor factorial design with mixed levels and three replications was selected in the experiment. The input variables are the peak temperature, the duration of time above solder liquidus temperature (TAL), solder alloy, component size, and thermal shock. The peak temperature and the TAL have three levels each and they are: the peak temperature at 12°C, 22°C, and 32°C above solder liquidus temperatures (or 230°C, 240°C, and 250°C for SAC 305 and 195°C, 205°C, and 215°C for SnPb), and the TAL at 30 seconds, 60 seconds, and 90 seconds. Therefore, there are nine reflow profiles for eutectic SnPb solder and nine for Sn3.0Ag0.5Cu (SAC305) solder. Test boards were assembled with four different sizes of pure tin plated surface mount chip resistors (1206, 0805, 0603 and 0402). Here 1206 means a component with a nominal length of 0.12 inch (3.0 mm) and a nominal width of 0.06 inch (1.5 mm). There were fourteen of each resistor size on each board, or 56 components total per board as shown in Figure 1. This resulted in the component size designed as a block. Three boards were assembled for each experimental run so a total of 54 boards were assembled (3 peak temperature x 3 TAL x 2 solder alloy x 3 replication).

Each board was cut into two identical pieces. The first half of the board stands for the initial time zero and the components on the half of the board were sheared right after assembly. The experimental results on the effect of reflow profile on shear force immediately after assembly were reported [8]. The other half of the test vehicles were then subjected to air-to-air thermal shock conditioning from -40 to 125°C with 30 minute dwell times (or 1 hour per cycle) for 500 cycles. The experimental matrix is listed in Table 1. The components were sheared using a Dage-series 4000 shear tester. For the components, solder paste, reflow profile development, assembly processes, and shear testing parameters please refer to the previously published paper [8].

Results

The solder joint shear force data were analyzed using analysis of variance (ANOVA). Three assumptions (normality, constant variance, and independence of the residuals) were checked in the ANOVA analysis. The residual plot for shear force (in gram) versus component size shown in Figure 2 indicates that the residual increases slightly as the component size increases. Thus the constant residual variance assumption is not satisfied and a transformation is needed. The square root transformation was found to be appropriate.

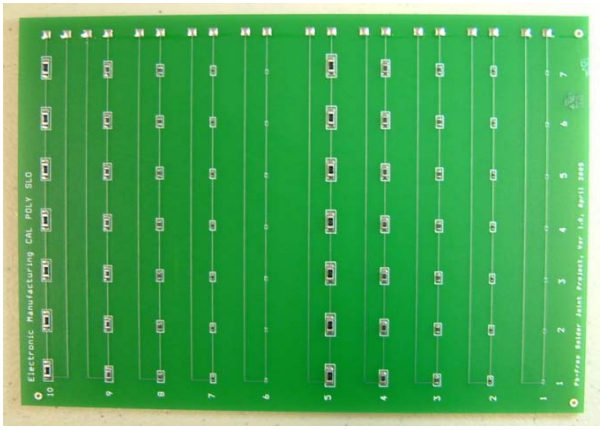

Figure 1: Test Vehicle

Table 1: Experiment matrix

Factors	Levels			
	1	2	3	4
Peak temperature above liquidus temperature (°C)	12	22	32	
TAL (sec.)	30	60	90	
Component size	1206	0805	0603	0402
Solder alloy	SnPb	SAC305		
Thermal shock	Before	After		

The ANOVA table for the square root of the solder interconnection shear force is summarized in Table 2. Though all the main factors have a statistically significant effect on the shear force at a 95% confidence level, the F-ratios indicate that the component size, the thermal shock, and the solder alloy are more significant factors compared to the peak temperature and the TAL. The interaction between the component size and the thermal shock is found to be significant as well.

Table 2: ANOVA for the Square Root of Shear Force

Source	Sum of Square	Df	Mean Square	F-Ratio	P-Value
Main Effects					
A: Peak Temperature	61.7	2	30.9	18.4	0.0000
B: TAL	33.9	2	16.9	10.1	0.0001
C: Component Size	41469	3	13823	8254.3	0.0000
D: Solder Alloy	893.2	1	893.2	533.4	0.0000
E: Thermal Shock	13137	1	13137	7844.7	0.0000
Interactions					
AB	3.8	4	0.9	0.6	0.6884
AC	9.5	6	1.6	1.0	0.4655
AD	19.2	2	9.6	5.7	0.0044
AE	7.2	2	3.6	2.1	0.1223
BC	24.8	6	4.1	2.5	0.0285
BD	21.2	2	10.6	6.3	0.0025
BE	3.6	2	1.8	1.1	0.3410
CD	400.6	3	133.5	79.7	0.0000
CE	3400	3	1133.	676.8	0.0000
DE	27.9	1	27.9	16.7	0.0001
Residual	172.5	103	1.67		
Total (corrected)	59685	143			

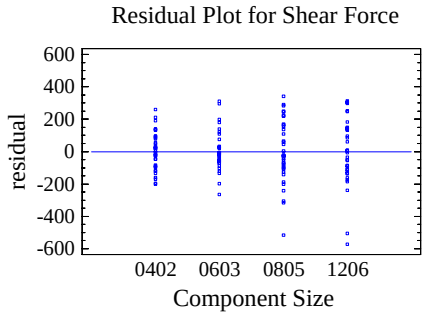

Figure 2: Plot of Residuals vs. Component Size

Effect of Peak Temperature and Time above Liquidus

Figure 3 shows that higher peak temperature (32°C above solder liquidus temperature, or 250°C for SnAgCu and 215°C for eutectic SnPb solder alloy) leads to higher shear force. Figure 4 shows that shorter time above liquidus results in higher shear force. As shown in Table 3, higher peak temperature and shorter time above liquidus means a faster cooling rate in the reflow process. The faster cooling rate results in fine microstructure of the solder joint. This may be the reason that higher peak temperature and shorter time above liquidus lead to high shear force. It should be pointed out again that the effects of the peak temperature and the TAL on solder joint shear force is smaller than that of thermal shock.

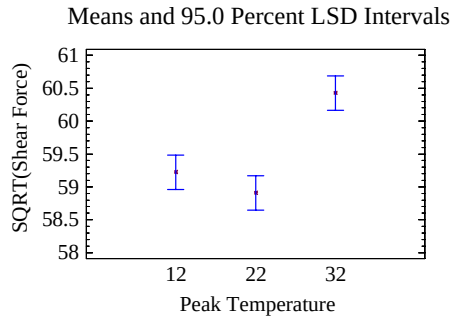

Figure 3: Effect of Peak Temperature on Shear Force

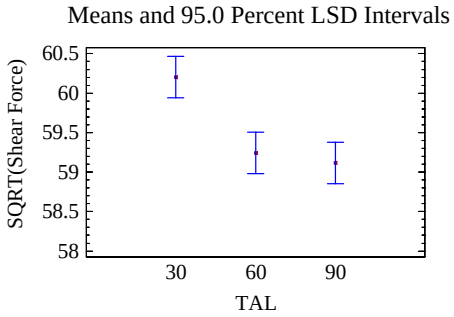

Figure 4: Effect of TAL on Shear Force

Table 3: Cooling Rate for Different Reflow Profiles

Peak Temperature above the solder liquidus point (°C)	TAL (sec.)	Cooling rate for SnPb (°C/sec)	Cooling rate for SAC305 (°C/sec)
12	30	2.7	3.1
12	60	2.2	2.5
12	90	2.3	2.1
22	30	2.7	3.0
22	60	2.2	2.4
22	90	2.2	2.0
32	**30**	**2.9**	**3.6**
32	60	2.3	2.5
32	90	2.4	2.2

Effect of Component Size and Solder Alloy

Figure 5 shows that the shear force increases with the size of the component. This is expected because the shear force equals to the shear strength of solder alloy times the solder joint wetting area and larger components have a larger solder wetting area.

Figure 6 indicates that the SnAgCu solder joints have weaker shear strength than the SnPb solders. This result is consistent with Oliver, et al. [6], but different from Sampathkumar, et al. [9]. It should be pointed out that the shear strength of solder alloy depends on the microstructure of the solder joint, which can be influenced by the reflow profile. The published shear strength of eutectic SnPb bulk solder alloy is 45.5MPa and that of Sn3.8Ag0.7Cu alloy is 63.8 MPa [10]. But the shear strength result from bulk solder specimens may not represent the behavior of actual solder joints where the scale of the microstructure may have an effect [11]. Another possibility could be due to the fact that the wetting of SAC305 is reportedly worse than SnPb [6, 12].

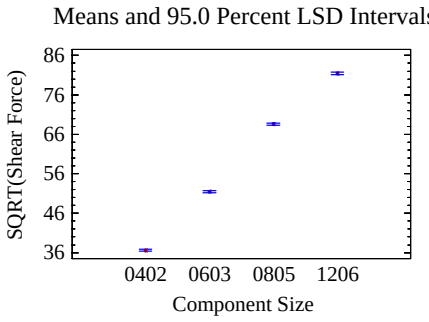

Figure 5: Effect of Component Size on Shear Force

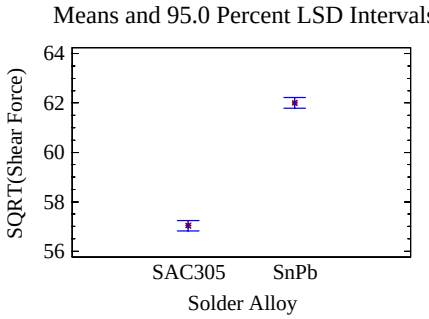

Figure 6: Effect of Solder Alloy on Shear Force

Effect of Thermal Shock

The interaction plots between the component size and the thermal shock data in Figures 7 and 8 shows that the shear force after thermal shock decreases more as the component size increases. This could be explained due to the larger thermal stress/strain in larger components during the thermal shock testing caused by the thermal expansion mismatch between the component and the board.

It is interesting to note that the shear force loss ratio (the shear force after thermal shock divided by the shear force before thermal shock) for the two solder alloys are different. Figure 9 shows that for small components, SAC305 solder retains more of its strength after heat shock, while for larger components, SnPb solder retains more strength. Table 4 lists the shear forces before thermal shock, after thermal shock, and the shear strength loss ratio for both SAC305 and SnPb solder joints. This result implies that the reliability of SnAgCu alloys outperform SnPb for small components and vice versa for large components. This conclusion is consistent with the thermal fatigue experimental results that suggested that SnAgCu alloys outperform SnPb at low strain applications and vice versa at high-strain amplitude applications [13-18].

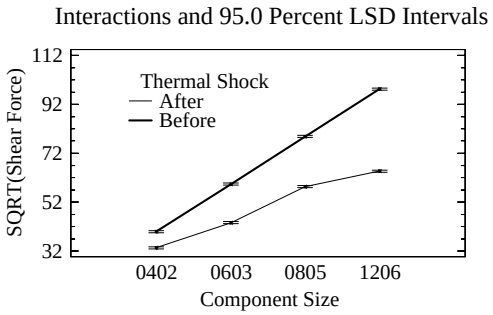

Figure 7: Interaction of Shear Force between Component Size and Thermal Shock

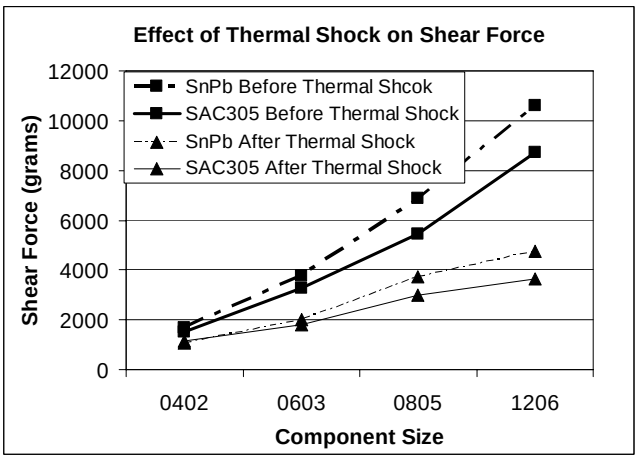

Figure 8: Effect of Thermal Shock on Shear Force

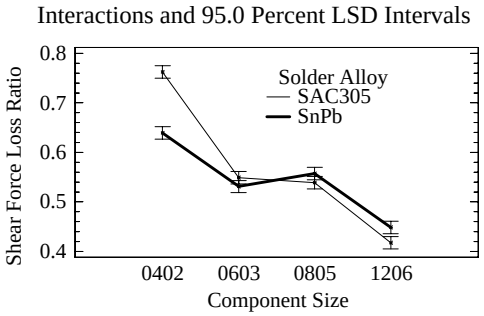

Figure 9: Interaction of Shear Force Loss between Component Size and Solder Alloy

Table 4: Shear Force Loss after Thermal Shock

Paste	Comp. Size	Shear Force (Newton)		Strength Loss (%)
		Before Thermal Shock	After Thermal Shock	
SAC305	0402	14.9	11.3	75.8
SAC305	0603	32.0	17.7	55.3
SAC305	0805	53.3	29.4	55.2
SAC305	1206	85.4	35.7	41.8
SnPb	0402	16.4	10.5	64.0
SnPb	0603	37.1	19.6	52.8
SnPb	0805	67.6	36.5	54.0
SnPb	1206	103.8	46.5	44.8

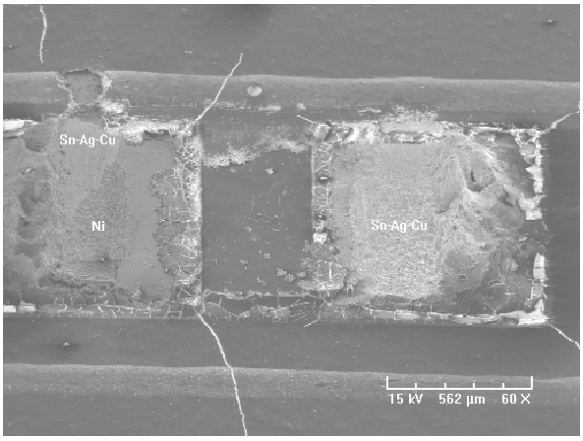

Figure 10: Fracture Surface of SAC305 Solder Joint after Thermal Shock

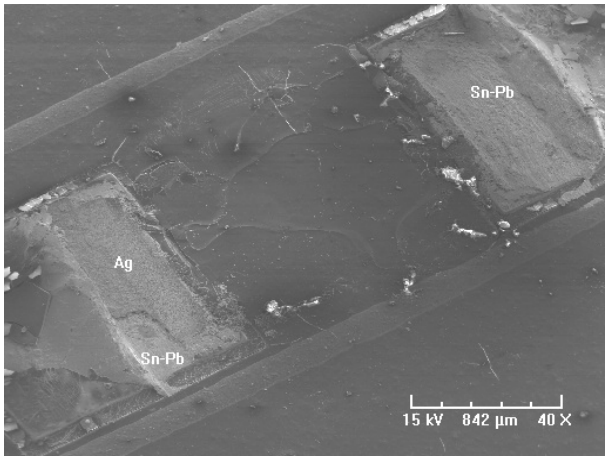

Figure 11: Fracture Surface of SnPb Solder Joint after Thermal Shock

Fracture Surface SEM/EDS Analysis

The fracture interfaces of SAC305 solder joints and SnPb solder joints after thermal shock are shown in Figure 10 and Figure 11, respectively. It was observed that the fracture interfaces vary for both SnPb joints and SAC305 joints. In most cases, the fracture occurred partially in the component metallization (Silver layer and or Nickel layer) and partially in the bulk solder joints, which is the same as the fracture surface of solder joints right after assembly [8]. In other cases, the fracture occurred in the bulk solder joints only.

Conclusion

The following conclusions can be drawn from this study:

1) Thermal shock (or loading condition) has significant effect on shear strength degradation of both SnPb and SnAgCu joints.

2) The effect of thermal shock on solder joint shear strength is much more significant than that of reflow profile.

3) Higher peak temperature and shorter time above liquidus lead to faster cooling rate and higher shear strength of solder joints.

4) The SnAgCu solder joints have weaker shear strength than the SnPb solders.

5) SnAgCu solder joint after thermal shock retains more of its shear strength than that of SnPb for small components (at low-strain amplitude applications) and vice versa for larger components (high-strain amplitude applications).

Acknowledgment

This work was sponsored by the Department of the Navy, Office of Naval Research, under Award #N00014-05-1-0855. The authors would like to thank Edward Clements for shear testing, Tzu-Chien Chou and Roger Jay at Solectron for SEM analysis. Special thanks to Flextronics International, DEK, Siemens, and Heller Industries for sponsoring the surface mount assembly line at Cal Poly, where the boards were assembled.

References

[1] C. Handwerker, "Transitioning to Lead-free Assemblies," *Printed Circuit Design and Manufacture*, March 2005, pp. 17-23.

[2] S.T. Nurmi, J.J. Sundelin, E.O. Ristolainen, and T. Lepisto, "The effect of PCB surface finish on lead-free solder joints," *Soldering & Surface Mount Technology*, Vol. 17, No. 1, pp. 13-23, 2005.

[3] K.J. Puttlitz, Handbook of Lead-Free Solder Technology for Microelectronic Assemblies, Edited by K. J. Puttlitz and K. A. Stalter, Marcel Dekker, Inc., New York, pp. 10, 2004.

[4] D. Shangguan, Lead-free Solder Interconnect Reliability, ASM International, 2005.

[5] B. Salam, C. Virseda, H. Da, N.N. Ekere, and R. Durairaj, "Reflow Profile Study of the Sn-Ag-Cu Solder," *Soldering and Surface Mount Technology*, Vol. 16, No. 1, pp. 27-34, 2004.

[6] J.R. Oliver, J. Liu, and Z. Lai, "Effect of Thermal Ageing on the Shear Strength of Lead-free Solder Joints, " Proceedings of the 2000 International Symposium on Advanced Packaging Materials, pp. 152-156.

[7] S. Bukhari, D.L. Santos, L.P. Lehman, and E. Cotts, " Continued Evaluation of the Effects of Processing Conditions and Aging Treatments on Shear Strength and Microstructure in Pb-free Surface Mount Assembly," Proceedings of the SMTA Pan Pacific Microelectronics 2005 Symposium.

[8] J. Pan, B.J. Toleno, T. Chou, and W.J. Dee, "The Effect of Reflow Profile on SnPb and SnAgCu Solder Joint Shear Strength," *Soldering & Surface Mount Technology*, Vol. 18, No. 4, 2006, pp. 48-56.

[9] M. Sampathkumar, S. Rajesnayagham, S.M. Ramkumar, and S.J. Anson, "Investigation of the Performance of SAC and SACBi Lead-free Solder Alloys with OSP and Immersion Silver PCB Finish," Proceedings of SMTA International 2005, Chicago, IL, USA, Sept. 25-29, 2005, pp. 568-575.

[10] T. Siewert, S. Liu, D.R. Smith, and J.C. Madeni, "Database for Solder Properties with Emphasis on New Lead-free Solders," NIST & Colorado School of Mines, Release 4.0, Feb. 2002, available at http://www.boulder.nist.gov/div853/lead free/solders.html

[11] B. Rodgers, B. Flood, J. Punch, and F. Waldron, "Determination of the ANAND Viscoplasticity Model Constants for SnAgCu," Proceedings of IPACK'2005, ASME InterPACK conference, San Francisco, CA, USA, July 17-22, 2005.

[12] S.V. Sattiraju, B. Dang, R.W. Johnson, Y. Li, J.S. Smith, and M.J. Bozack, "Wetting Characteristics of Pb-Free Solder Alloys and PWB Finishes," *IEEE Transactions on Electronics Packaging Manufacturing*, Vol. 25, No. 3, pp. 168-184, 2002.

[13] J. Pan, J. Wang, and D.W. Shaddock, "Lead-Free Solder Joint Reliability – State of the Art and Perspectives," *IMAPS Journal of Microelectronics and Electronics Packaging*, Vol. 2, No. 1, 2005, pp. 72-83.

[14] J.H. Lau, D. Shangguan, D. Lau, T. Kung, and R. Lee, "Thermal-Fatigue Life Prediction Equation for Wafer-Level Chip Scale Package (WLCSP) Lead-Free Solder Joints on Lead-Free Printed Circuit Board (PCB)," Proceedings of IEEE Electronic Components and Technology Conferences, Las Vegas, May 2004, pp. 1563-1569.

[15] J.H. Lau, N. Hoo, R. Horsley, J. Smetana, D. Shangguan, D. Dauksher, D. Love, I. Menis, and B. Sullivan, "Reliability Testing and Data Analysis of Lead-Free Solder Joints for High-density Packages," *Soldering & Surface Mount Technology*, Vol. 16, No. 2, pp. 46-68, 2004.

[16] S.T. Nurmi, J.J. Sundelin, E.O. Ristolainen, and T. Lepisto, "The influence of multiple reflow cycles on solder joint voids for lead-free PBGAs," *Soldering & Surface Mount Technology*, Vol. 15, No. 1, pp. 31-38, 2003.

[17] J.C. Suhling, H.S. Gale, R.W. Johnson, M.N. Islam, T. Shete, P. Lall, M.J. Bozack, J.L. Evans, P. Seto, T. Gupta, and J.R. Thompson, "Thermal Cycling Reliability of Lead-Free Chip Resistor Solder Joints," *Soldering & Surface Mount Technology*, Vol. 16, No. 2, pp. 77-87, 2004.

[18] M. Farooq, L. Goldmann, G. Martin, C. Goldsmith, C. Bergeron, "Thermo-Mechanical Fatigue Reliability of Pb-Free Ceramic Ball Grid Arrays: Experimental Data and Lifetime Prediction Modeling," Proceedings of the 2003 IEEE/CPMT Electronic Components and Technology Conference, New Orleans, LA, pp. 827-831.

Biographies

James Webster was an undergraduate student majoring in Industrial Engineering at California Polytechnic State University, San Luis Obispo, CA 93401 USA. He is now with Raytheon, working as a program scheduler at, 2000 E. El Segundo Blvd., El Segundo, CA 90245 USA (e-mail: jamespwebster@gmail.com).

Jianbiao Pan, Ph.D. (M'97-SM'05) received the B.E. degree in mechatronics from Xidian University, Xian, China, in 1990, the M.E degree in manufacturing engineering from Tsinghua University, Beijing, China, in 1996, and the Ph.D. in industrial engineering from Lehigh University, Bethlehem, PA, in 2000.

He is an assistant professor in the Department of Industrial and Manufacturing Engineering at California Polytechnic State University (Cal Poly), San Luis Obispo, CA. Prior to joining Cal Poly, he worked at the optoelectronics center of Lucent Technologies/Agere Systems as a member of technical staff. His research interests are in microelectronics packaging, electronics assembly, lead-free soldering, design of experiments, and statistical process control.

Dr. Pan is a senior member of SME and IEEE, a member of Sigma Xi. He is a recipient of the 2004 M. Eugene Merchant Outstanding Young Manufacturing Engineer Award from SME.

Brian J. Toleno, Ph.D., is with Henkel Technologies, 15350 Barranca Parkway, Irvine, CA 92618 USA (e-mail: brian.toleno@us.henkel.com)